

OAK RIDGE
NATIONAL LABORATORY

MANAGED BY UT-BATTELLE
FOR THE DEPARTMENT OF ENERGY

Kinetic Testing of Nitrate-Based Sodalite Formation over the Temperature Range of 40 to 100°C

August 2001

A. J. Mattus
C. H. Mattus
R. D. Hunt

ORNL/TM-2001/117

Chemical Technology Division

**Kinetic Testing of Nitrate-Based Sodalite Formation over
the Temperature Range of 40 to 100 °C**

A. J. Mattus
C. H. Mattus
R. D. Hunt

Oak Ridge National Laboratory
P. O. Box 2008
Oak Ridge, Tennessee 37831-6221

Date Published: August 31, 2001

Prepared by the
OAK RIDGE NATIONAL LABORATORY
Oak Ridge, Tennessee 37831-6285

managed by
UT-BATTELLE, LLC

for the
U.S. DEPARTMENT OF ENERGY
under contract DE-AC05-00OR22725



LOCKHEED MARTIN ENERGY RESEARCH LIBRARIES

3 4456 0452897 5

TABLE OF CONTENTS

LIST OF TABLES	v
LIST OF FIGURES	vii
EXECUTIVE SUMMARY	ix
1. INTRODUCTION	1
2. EXPERIMENTAL	3
2.1 EQUIPMENT AND PROCEDURE	3
2.2 SOLUTION PREPARATION AND USE	5
2.3 SIMULANT COMPOSITION	6
2.4 PREPARATION OF SODIUM SILICATE SOLUTION	7
2.5 PREPARATION OF CHEMICAL REAGENTS	8
2.6 PREPARATION OF SALT SOLUTION	8
3. ANALYTICAL METHODS	8
3.1 X-RAY DIFFRACTION (XRD)	8
3.2 INDUCTIVELY COUPLED PLASMA (ICP) EMISSION SPECTROSCOPY	9
4. RESULTS	9
4.1 EXPERIMENTAL DATA	9
4.2 ALUMINOSILICATE FORMATION KINETICS	10
4.2.1 Reactions at 40°C	10
4.2.2 Reactions at 60°C	10
4.2.3 Reactions at 80°C	11
4.2.4 Reactions at 100°C	12
4.3 TEST FOR SECOND-ORDER REACTION KINETICS	13
4.4 ACTIVATION ENERGY FOR ALUMINOSILICATE CRYSTALLIZATION	15
4.5 RATE CONSTANTS AT HIGHER EVAPORATOR OPERATING TEMPERATURES	16
4.6 REACTION INDUCTION PERIODS	17
4.7 REACTOR SCALING AND DEPOSITION OBSERVATIONS	18
4.7.1 Using Aluminum Concentrations in Excess of Silicon	19
4.7.2 Using Silicon Concentrations in Excess of Aluminum	19
4.8 ZEOLITE A PRECURSOR PHASE	20
4.9 USING CARBON BLACK AS A SEED	21
4.10 A KINETIC TEST AT 100°C	24
5. CONCLUSIONS	25

TABLE OF CONTENTS (Continued)

6. RECOMMENDATIONS 26

7. REFERENCES 27

LIST OF TABLES

Table 1. Composition of the simple salt solution feed representing Tank 43H	6
Table 2. Composition of glass Frit 200	7
Table 3. Reagent purity and lot information	8
Table 4. Desilication reaction induction periods	17

LIST OF FIGURES

Figure 1. Experimental setup and associated equipment	4
Figure 2. Mole fraction consumption of reactants at Al:Si = 1 at 60°C	11
Figure 3. Mole fraction consumption of reactants at different Al:Si ratios at 80°C	12
Figure 4. Mole fraction consumption of reactants at 0.1 M Al and 0.1 M Si at 100°C	13
Figure 5. Second-order reaction test plot for aluminosilicate formation at 100°C and an Al:Si molar ratio of 1:1 (0.1 M Al:0.1 M Si)	14
Figure 6. Arrhenius activation energy determination for unseeded desilication reactions	15
Figure 7. XRD spectra showing the conversion of Zeolite A into nitrate-based sodalite	21
Figure 8. SEM photomicrograph showing sodalite growth on carbon black surfaces	23
Figure 9. SEM photomicrograph of unused carbon black	23
Figure 10. Concentration versus time for a reaction at 100°C (Al:Si = 1) showing an approach to equilibrium after 4 h.	24

EXECUTIVE SUMMARY

The focus of this study was the desilication kinetics of a Savannah River Site (SRS) tank farm 2H simulant over the temperature range of 40 to 100°C. Results showed that the formation of nitrate-nitrite-based sodalite over aluminum-to-silicon (Al:Si) molar ratios ranging from 1:1 to 20:1 exhibited overall-second order kinetics. The Arrhenius apparent activation energy associated with the crystal growth process of the sodalite was determined to be 35 kJ/mol over the temperature range investigated. Second-order rate constants were extrapolated to the 2H evaporator working temperature of ~130°C and were found to be 0.012 L mol⁻¹ s⁻¹. At this operating temperature, the half-life of a limiting reactant with a 0.1M feed would be 14 min.

The rate of sodalite formation was found to be at a maximum at Al:Si molar ratios of 1:1 (0.1 M Al and 0.1 M Si) and to increase with increasing temperature. Use of Al:Si molar ratios of 20:1 resulted in no reaction for up to 130 h, probably due in part to having reactant concentrations close to the solubility limit of the nitrate-nitrite-based sodalite, thereby minimizing the thermodynamic driving force. A test performed at 100°C with a reactant molar ratio of 1:1 was nearly complete (90%) in only 4 h. Equilibrium appeared to have been achieved during the last 3 h of the 7-h test. From analytical data collected during the last 3 h, a solubility product constant (k_{sp}) of $2.6 \pm 0.1 \times 10^{-4} \text{ M}^2/\text{L}^2$ was calculated for the nitrate-nitrite-based sodalite.

Sodalite scale formation has consistently been found to form on vessel surfaces at most Al:Si ratios and temperatures that were evaluated, especially when the aluminum concentration equals that of the silicon in solution where it is most pronounced. However, it has also been found from tests in which the silicon concentrations exceed that of aluminum at 80°C, and at an Al:Si ratio of 0.05 (0.005 M Al and 0.1 M Si), that the precipitation proceeds without visible scale formation. All solids appeared to form in the bulk of the solution instead of on vessel surfaces.

A reaction induction period was observed in most of the experiments except for those performed at 100°C. At a temperature of 80°C and Al:Si molar ratios of both 1:1 (0.1 M Al and 0.1 M Si) and 2:1 (0.1 M Al and 0.05 M Si), the induction periods were 1 and 5 h, respectively. Tests performed at 60°C followed the same trend in that induction periods became longer, while results obtained from tests performed at 40°C were erratic. Generally as the reaction temperature increased, the induction period decreased.

Utilizing x-ray diffraction (XRD), nearly all solid phases that formed either in the bulk solution or attached to reaction vessel surfaces, were shown to be a nitrate-nitrite-based sodalite. It has also been shown that the mineral-phase zeolite A initially forms and then transforms into the sodalite phase, even at temperatures as low as 40°C. At higher temperatures, the transition is fast enough that it can be missed, whereas at 80°C, solids in the bulk of the solution were shown to transition during the first 3 h of the reaction.

Solids were shown to build on and tenaciously adhere to reaction vessel surfaces (304-L stainless steel).

The mixing propeller used in this work pushed liquid in the reaction vessel downward, while stirring at 250 rpm. As a result, the walls always appeared to remain clean in the same plane as the propeller and just above, as well as immediately below the propeller on the bottom

surface. The reason for this is not entirely clear, but may relate to the turbulence profile created inside the reaction vessel. Previous observations of scale growth and deposition on vessel surfaces have indicated that particles formed in the solution appear to preferentially form where they impact the surface of the vessel wall at a steep angle. Upon adhering to the surface, the solids seem to grow laterally into a sheet that covers the surface.

One test using carbon black as a seed material was performed in an attempt to investigate preferential growth and formation of aluminosilicate solids in the bulk of the solution rather than on vessel surfaces. This test was performed at 80°C and at an Al:Si molar ratio of 1 (0.1 M Al and 0.1 M Si). At the start of the reaction, an equivalent 2.4 kg carbon black per 1000 L of simulant was added and became wetted after about 5 min of mixing. After 6 h, the surfaces of the vessel were free of solids under conditions which normally produce the maximum amount of solids on vessel surfaces. The amount of carbon used was conservative and likely exceeded that which might be necessary. This seed material was of special interest since it might be expected to oxidize to CO₂ in the melter cold cap region.

1. INTRODUCTION

Since 1997 the Savannah River Site (SRS) has been plagued with pipeline plugging problems associated with the formation of aluminosilicate mineralization, which has recently lead to the shut down of the 242-16H (2H) evaporator system. This evaporator's primary function was to reduce the volume of the SRS high-level waste solution stored in storage tank 43H. The concentrate from this evaporator flows through a gravity drain line to tank 38H. The evaporation reduces the volume of the high-level waste by 25 to 30% and the volume of the low-salt waste by approximately 90%.¹ The high-salt waste typically contains high concentrations of aluminum and very low concentrations of silicon. The low-salt waste which originates as a recycle stream from the Defense Waste Processing Facility (DWPF) has, by contrast, high concentrations of silicon and low concentrations of aluminum. The subsequent combination of these two streams has led to serious problems for the 242-16H evaporator. During July 1997, a drain line to tank 38H became plugged with a nitrate-based sodalite. More recently, the evaporator has been inoperable since January 2000 due to similar excessive scaling.²

The drain line was unplugged using a water jet, and evaporator solid dissolution studies were undertaken by Wilmarth.^{3,4} The nitrate-based sodalite was found to not be amenable to dissolution in caustic or oxalate solution but rather in dilute sulfuric and nitric acid, the latter of which is compatible with the 304-L stainless steel and Hastelloy G-30 metals of construction.⁵ During this time, it was discovered that tank 2H contained solids that were comprised of 6% uranium which had been enriched to 2.4%. Concern regarding the possibility of exceeding criticality limits in the tanks and the evaporator prompted the Department of Energy (DOE) to suspend evaporator operations.

The 242-16H (2H) evaporator is part of the H-Area tank farm. The evaporator is 8 ft in diameter and 16.5 ft tall, with an operating capacity of ~1950 gal,⁵ a design pressure of 15 psig, and an upper operating temperature of 160°C. The evaporator has a conical bottom for more efficient removal of concentrated waste.

Waste which is continuously fed from Tank 43H can be heated by two sources inside the evaporator, the warming coils and the steam tube bundle, although the tube bundle is used primarily for this purpose. The 150-psig steam passing through the bundle normally heats the solution to 130°C. The warming coils are used during shutdown and during desalting or descaling operations.⁵

The tank farm evaporators ran with few operational problems for a period of approximately 40 years. During this time, any buildup of salt was readily washed out using well water. However, more serious scaling problems arose in 1997 and 1998 when scale samples were shown to contain aluminosilicates, corresponding to the relatively insoluble nitrate-based sodalite mineral. This material was found to be tenaciously attached to surfaces inside the evaporator and could not be removed as easily as in the past with well water.

More troubling than the scaling itself was the realization that sodium diuranate had precipitated with the scale and it had become enriched.⁶ Uranium in the range of 3 to 7.4 wt% was discovered with average enrichment of approximately 3%. Because of the criticality concern, the 2H evaporator was shutdown and locked out in January 2000.⁵ Recent calculations indicate that approximately 3500 kg of scale deposit and 9 kg of fissile ²³⁵U are present in the

evaporator. The fissile uranium is approximately four times the minimum critical mass of 2100 g ^{235}U for 3% enrichment. For this reason, acid-cleaning procedures will include the addition of depleted uranium to dilute the enriched uranium into a safe range.

The presence of glass frit in the feed tank sludge as well as in the recycle stream from DWPF has contributed to the formation of problematic aluminosilicate, a material which has also presented major scaling problems for the nearly 100-year-old Bayer process.⁷ In that process, the scaling problem originates from the presence of kaolinite, $\text{Al}_2\text{Si}_2\text{O}_5(\text{OH})_4$, and quartz SiO_2 , in the bauxite process feed.⁸ Many aspects of the Bayer process chemistry and important physico-chemical parameters are analogous to those of the evaporator problem at the SRS.

The problem of scaling in industry is most often related to heat transfer surfaces becoming coated in boilers, desalination/distillation plants, and many types of evaporators. In most cases, industry has not been able to solve the problem entirely and must periodically resort to acid cleaning or solutions containing complexing agents or chelants to descale.⁸⁻¹⁰

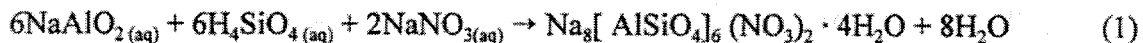
The complexity of the scale-formation problem even extends to the atomic scale where grain boundaries on metal surfaces interact or aid in scale formation.¹¹ Generally the existence of an oppositely charged surface oxide on metal that aids in attracting negatively charged reactant or product particles is considered plausible. One may speculate that product particles (or crystals) may be surrounded by a still-evolving gel phase that moves with the particle and upon contact with the 304-L stainless steel surface, if positively charged, facilitates the formation of a weak electrostatic attachment, which later forms a strong covalent bond through surface species such as $\text{Fe}(\text{OH})^+$.¹²

Industry relies on several different methods to control scaling, some of which are briefly summarized as follows:

1. Mechanical means including thermal shock have sometimes been used on submerged-tube evaporators.
2. The addition of seed materials to facilitate and speed growth in the bulk of the solution rather than on heat exchange surfaces is another approach.
3. Ion-exchange methods have been used to remove certain chemical species that aid in scale growth.
4. Polyphosphate-based chemicals are added at doses in the range of 2–5 ppm. The exact mechanism of scale abatement using this additive is not entirely understood.
5. Simple pH adjustment is used to effect a change in the solution chemistry, such as to remove carbonate from water as carbon dioxide.
6. A family of high-temperature polymers are sometimes added in the range of 3–8 ppm so as to produce a lattice distortion in the solid and subsequently result in the production of a non-adhering scale due to this distortion.⁹

With the exception of the Bayer process, problems at the SRS result from conditions that are not very common to industry. In addition, solutions to these problems are limited by what can be added to the waste feed solutions. Amorphous frit for the melter which is present in the feed tanks is the ultimate source of the scaling problem. According to the experimental results of Wilmarth, the frit dissolves to a limited extent in the feed tank, especially when the sludge is

turned over.¹³ Upon being fed to the evaporator, its dissolution and subsequent conversion to sodalite is nearly quantitative and occurs in less than 4 h, which is thought to be the residence time inside the 2H evaporator. According to Wilmarth, a kilogram of Frit 200 (70% SiO₂) produces 2.1 kg of the sodium aluminosilicate. Together with silica from the DWPF recycle stream, silicate is being continuously replenished, thus requiring a better understanding of the reaction kinetics as well as the mechanism(s) involved in wall deposition and scaling. A general equation for the formation of the problematic nitrate-based sodalite, simplistically omitting metastable intermediate gels or a solid precursor phase, is depicted in Eq. (1) :



As might be expected based upon the waste stream composition, and confirmed through XRD analysis, the sodalite formed actually contains equal molar quantities of nitrate and nitrite despite reference to a nitrate-based sodalite.

At present the plan to make the 2H evaporator operational in the future involves the use of a dilute nitric acid and depleted uranium cleaning solution as formulated by Wilmarth.² A periodic shutdown of the evaporator for cleaning purposes will be necessary, and each cleaning is expected to require several batches to effect complete dissolution of the aluminosilicate-based scale. In addition, since it has been shown through XRD analysis of sodalite mineralization that the mineral is actually both nitrite and nitrate based, it is expected that a lot of gaseous mixed oxides of nitrogen will be produced upon contact with acid. That is, the nitrite component will readily decompose to form the mixed oxides of nitrogen and the heat associated with the acid-base reaction may promote additional decomposition of nitrate, depending upon the concentration of the acid. The final acidic solutions will also require caustic neutralization, thereby producing more heat prior to movement to Tank 42 and possibly more NO_x.¹⁴

2. EXPERIMENTAL

2.1 EQUIPMENT AND PROCEDURE

All kinetics tests were performed in a constant-temperature water bath which was maintained within 0.25°C of the programmed temperature. The bath temperature was checked periodically against a National Institute of Standards and Technology traceable thermocouple-based meter that has been certified as being calibrated through January 3, 2002. A Lightnin mixer with an electronic rpm display was used to stir the solutions at 250 rpm. Distilled water was used in the bath during most of the testing, but was replaced with silicon oil for tests conducted at temperatures of 100°C. The bath and mixer arrangement and other associated equipment are shown in Fig. 1(a-c).

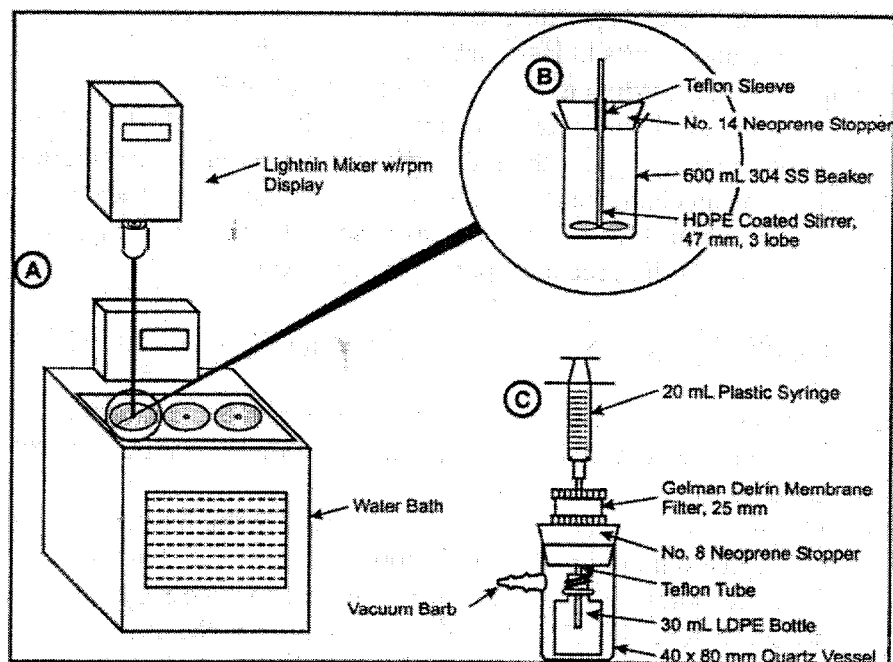


Fig. 1. Experimental setup and associated equipment.

The bath opening was modified by adding a steel plate with three openings to allow for the use of three reactors simultaneously. Initially two positions were set aside for heating the two reactant solutions (salt and silicate based), after which they were combined into the third 600-mL stirred stainless steel (SS) vessel. The reaction vessels were manufactured by Polar, Inc., and were made of polished 304-L SS. The vessels were straight walled with a lip that caught the top of the plate and allowed the vessel to hang low enough in the water or silicon oil that the solution inside (450 mL) was always at or below the liquid level in the bath.

The solution was stirred using a high-density polyethylene (HDPE)-coated stirrer and propeller with three 45° lobes which turned clockwise at 250 rpm during use. This direction of rotation forced the vessel solution downward. The shaft of the propeller passed through a close-fitting Teflon tube, centered in the top of a number 14 neoprene stopper, which fit snugly in the top of the reaction vessel. On top of the stopper was placed a 5-lb slotted hanging-scale weight of the same diameter as the stopper, which ensured that the seal with the vessel was always tight. The 47-mm-diam mixer propeller was always placed 2 cm above the bottom of the reaction vessel by aligning a mark on the mixer shaft with the opening of the chuck, and the mixer motor was aligned with a mark on its support rod. The reaction vessel and mixer arrangement are shown in Fig. 1(b); the slotted weight is not shown.

Liquid samples of the reactant solution were periodically removed, with sample times being dictated primarily on the basis of the operating temperature selected and discussions with Savannah River Technology Center (SRTC) staff who had run similar tests over the past few years. Based on some early practice tests, it was found that when a lot of solids were suspended

in solution, it became more difficult to force the reactor solution through the syringe filter used. Under such conditions, the solution inside the 20-ml plastic syringe might have cooled as a result of the long filtering delay, and thereby altering the solution composition due to possible unwanted precipitation. To overcome this limitation, a glass water jacket was constructed that tightly fit the syringe. Water from the bath was constantly pumped through the jacket to maintain the temperature inside the syringe at the same temperature as in the bath. It was later determined that in most cases, the filtration of 10–12 mL of solution was rapid and in the range of 15 s, a time in which cooling became less important. As a result, the heated jacket was rarely used but always remained available nearby with bath water flowing through it.

The apparatus used for solution filtration is schematically shown in Fig. 1(c). Upon removing the weight and neoprene stopper from the reaction vessel, the plastic syringe with a Luer lock end was placed just below the surface of the constantly stirred solution and between 10 to 12 mL of solution was removed. The syringe was then attached to the top of a Delrin plastic filter (VWR 28144-109, 2000 catalog), which contained a 0.2- μm nylon filter with a Viton O ring. The filter also contained a Luer lock connection. The end of the filter was attached to the top of a drilled number 8 neoprene stopper with a Teflon tube extending about 3 cm below the stopper and into a preweighed 30-mL polyethylene bottle placed inside a 40- × 80- mm quartz vessel made for these tests. This vessel was attached to a vacuum source through the vacuum barb on its side, thus allowing a vacuum to be pulled at the same time the syringe plunger was being pushed to force the solution through the filter. In this way, both the pressure inside the syringe and the vacuum on the other side of the filter facilitated rapid filtration. The vacuum was not used in tests at or above temperatures of 100°C because the solutions would flash inside the quartz vessel.

Upon filtering the sample, the apparatus was opened and the sample bottle sealed and weighed to correct for the amount of solution removed from the reaction vessel with time. If there was enough solid in solution to enable a solid sample to be recovered from the filter, a clean syringe was filled with 20 mL of distilled water to wash the electrolyte out of the solids on the filter. The filter was reattached to the top of the Delrin plastic filter, and water was then forced through the filter into the empty quartz vessel below, generally without the aid of a vacuum.

Following the washing step, the apparatus was dismantled and the two halves of the Delrin filter were screwed apart to expose the filtered solids. The nylon filter with solids attached as a filter cake was carefully removed using laboratory tweezers, placed in marked petri dishes, and then put in a 52°C drying oven for a minimum of 12 to 24 h. When searching for the presence of gibbsite, some samples were dried a second time at 100°C for 72 h to force dehydration and crystallization of any amorphous gibbsite. Dried solids were found to be very friable and were ground in an agate mortar prior to storage in vials.

2.2 SOLUTION PREPARATION AND USE

Chemical characterization at various levels inside feed tank 43H was conducted to formulate the simulant used in these kinetic tests.¹⁵ The concentration range of sodium, aluminum, and silicon was used to generate four simulant options. Of these options, the simulant

with a total sodium concentration of 6 M was chosen for this study. The working solution was prepared in two parts, a salt solution containing the aluminum and other salts and a sodium silicate-based solution made using Frit 200. The two solutions would be separately heated to the desired reaction temperature and then combined at the start of the test, producing a final solution with the desired Al:Si ratio.

All solutions prepared in this study were stored in screw-top polypropylene volumetric flasks due to their high alkalinity and never exceeded 1 L in volume. This minimized the potential for changes in both the salt and silicate-based solutions, and upon using 450 mL of solution in each test, a fresh solution was often prepared.

2.3 SIMULANT COMPOSITION

The resultant solution composition produced after combining the salt solution with the silicate solution was kept as constant as possible. Only the sodium concentration varied slightly. The simulant composition showing the initial aluminum concentration of 0.133 M is presented in Table 1; this concentration was changed to achieve the desired Al:Si ratios.

Table 1. Composition of the simple salt solution feed representing Tank 43H

Species	Concentration (M)
Sodium	6.000
NaOH	4.000
NaNO ₃	1.000
NaNO ₂	1.000
Al(NO ₃) ₃ · 9H ₂ O	0.133

The salt solution was prepared in such a way that the sodium hydroxide from the silicate solution would be accounted for in producing a final caustic concentration of 4 M (as shown in Table 1) after the two were combined. However, since the aluminum nitrate nonahydrate has nitrate with it, its concentration must be corrected for in the total. In addition, since the aluminum cation is acidic, upon contacting the solution it will consume 4 mol of hydroxide, Al(OH)₄⁻, which must be accounted for in the total sodium hydroxide concentration (i.e., that from salt solution and that from the added silicate solution). The preparation of the salt solution required that the sodium nitrite be added last, after the alkalinity had neutralized the acidic aluminum cation; otherwise, the nitrite would decompose into brown NO_x fumes. In earlier tests, the aluminum concentration was held at 0.1 M and the silicon was reduced from 0.1 M down to 0.005 M so as to obtain Al:Si ratios of 1:1, 2:1, and 20:1. A solution comprised of 4 M NaOH was used for dilution when necessary. The aluminum concentration of the 0.1 M salt solution shown in the table was initially prepared at 0.2 M so that when mixed with an equal volume of

0.2 M silicate solution, a solution containing both 0.1 M aluminum and silicon resulted (Al:Si = 1).

2.4 PREPARATION OF SODIUM SILICATE SOLUTION

The silicate-based solution was prepared using the same glass frit as that used in the vitrifier at the SRS. The preparation required that 20 g of Frit 200 be mixed with 160 g of NaOH and water and heated in a stirred stainless steel vessel, using a Teflon-coated magnetic stir bar, for 24 h at 100°C. The composition of Frit 200 is provided in Table 2. The steel vessel was covered, and the lid was equipped with a reflux condenser with 16°C water passing through it. After 24 h, the vessel was cooled to near room temperature in a water bath. The solution was then filtered through Whatman 40 filter paper and rinsed into a 1-L polypropylene volumetric flask. Distilled water was added until the total volume reached the 1-L mark. An aliquot was then submitted for inductively coupled plasma (ICP) analysis for silicon concentration. Very consistent results of 0.2 M SiO₂, 3.66 M OH⁻, and 4.06 M Na⁺ with a density of 1.16 g/mL at 24°C were obtained. When lower concentrations of SiO₂ were required, the solution was diluted with 4 M NaOH. Both the free hydroxide and sodium composition were calculated by the use of a spreadsheet. Attempts were made to titrate the free hydroxide with standard hydrochloric acid to the methyl orange end point with an autotitrator, but results, although close to those calculated, were generally high, probably due to the carbonate present in the food-grade sodium hydroxide used. Using this method, the titration is ended just before silicate begins to protonate.¹⁶ The silicon was obtained by ICP, and the sodium usually agreed very closely with the calculated sodium concentration.

An Excel spreadsheet was used to balance the desired amounts of cations and anions and account for added or consumed components to yield the desired Al:Si to silicon ratios in the final solution upon being combined with the salt solution. After all solution densities had been determined, solutions were combined by weight to minimize error.

Table 2. Composition of glass Frit 200

Component	wt%
SiO ₂	70
B ₂ O ₃	12
Li ₂ O	5
Na ₂ O	1
MgO	21

2.5 PREPARATION OF CHEMICAL REAGENTS

The purest chemical reagents practically available were used in preparing both silicate and salt solutions. Large containers of reagents were purchased to avoid changes in lot number. Table 3 shows the reagents used, their purity, and their associated lot numbers.

Table 3. Reagent purity and lot information

Reagent	Manufacturer	Grade and Purity	Lot #
NaNO ₃	EM Science	ACS (mp 306°C)	08711CU
NaNO ₂	EM Science	GR (97% min)	39099917
Al(NO ₃) ₃	EM Science	GR (98–102%)	37325925
NaOH	Mallinckrodt	NF (99.2%)	7680T28469

2.6 PREPARATION OF SALT SOLUTION

The salt solution was prepared separately and mixed with the silicate solution in equal volumes (based upon weight). A spreadsheet was used to resolve the amount of salts needed to produce a simulant at the desired Al:Si ratio, as shown in Table 1. In all tests, 225 mL of salt solution was mixed with 225 mL of the silicate-based solution in the reaction vessel following preheating, producing a final volume of 450 mL in each test.

3. ANALYTICAL METHODS

3.1 X-RAY DIFFRACTION (XRD)

Solid samples removed during the course of this study were filtered onto 0.2- μ m nylon filters and washed well with distilled water by forcing a 20-mL syringe of water through the solids on the internal filter to remove traces of electrolyte that might affect the XRD spectrum. Washed solids were placed on petri dishes and put in a drying oven at 52°C where they remained for a minimum of 12 h. When testing for the presence of gibbsite, which might exist in the solids as an amorphous phase, the solids were dried at 100°C for 72 h prior to XRD analysis. All solids for XRD were ground in an agate mortar and then sealed in glass vials prior to analysis.

XRD analysis was conducted using an XDS 2000 diffractometer from Scintag, Inc. (USA). The Jade 6 XRD pattern processing software manufactured by Materials Data, Inc., was used for data interpretation and to identify peaks over a 2-theta range of 4 to 40 degrees at a continuous scan rate of 1 degree per minute.

3.2 INDUCTIVELY COUPLED PLASMA (ICP) EMISSION SPECTROSCOPY

Liquid samples removed from the reaction vessel for silicon and aluminum analysis were kept in 20-mL polyethylene bottles and generally contained between 10 to 12 mL of sample each. Most samples were analyzed within 2 days and were stored at room temperature. For tests performed at higher temperatures and higher Al:Si ratios, samples were quickly stored in a refrigerator at 2°C to minimize any further reactivity.

Liquid samples were analyzed from both nitric acid-based matrices as well as those that were nitric, hydrochloric and hydrofluoric acid based, with the latter producing less erratic results for sometime problematic silicon. Analyses from the nitric-hydrofluoric matrix consistently gave somewhat higher results compared with nitric acid alone, and fluoride appeared to minimize silicate loss due to precipitation upon dilution and acidification. Aluminum results were nearly always consistent and rarely erratic.

The ICP used was a Model 61E Trace Analyzer from Thermo Jarrell Ash that is a simultaneous plasma emission spectrometer. It consists of three modular components: (1) a computer-controlled 0.75- μm polychromator with a fully automated ICP emission source; (2) a floor-mounted power unit that provides power to all other components and accessories, with the exception of the polychromator vacuum pump; and (3) a data acquisition center that includes the host computer and a printer.

The emission source for the ICP 61E is an argon plasma. The ICP source is powered by a 2-kW crystal controlled radio frequency (RF) generator operating at 27.12 MHz. The output from the RF generator is coupled to a water-cooled copper induction coil that is wrapped around the outside of a quartz torch assembly. Argon gas flows through the torch assembly at all times.

4. RESULTS

4.1 EXPERIMENTAL DATA

Analytical data were initially graphed versus time, and results were used to determine if an induction period existed prior to fitting data to standard integrated forms for first- or second-order reactions by trial and error to obtain the best fit. For those reactions in which an induction period was present, the zero time was shifted to the point at which the reaction was initiated. It was found that tests in which the Al:Si molar ratios were 1:1 (0.1 M Al and 0.1 M Si) could be described using a second-order fit of the data, while those at other ratios best fit pseudo first-order kinetic relationships. For tests in which the molar ratios were 1:1, either aluminum or silicon could be used, with aluminum as the preferred choice since random analytical problems with silicon sometimes were encountered. Although many different means for describing kinetic data exist for such systems, such as the half-life method, initial rate, differential forms, and integrated forms, the latter method was relied upon. Where both reactants start at the same concentration, tests with Al:Si molar ratios of 1:1 (0.1 M Al and Si 0.1 M) were used.

4.2 ALUMINOSILICATE FORMATION KINETICS

The acquisition of kinetic data that lends itself to justifiable comparison may depend on many conditions which could affect the end results, such as sample storage prior to chemical analysis, filtration efficiency, or simply differences in procedure. In all the kinetic tests performed, this work has focused on maintaining consistency in how the tests were conducted to ensure comparability. The only known major difference is that in work at 100°C, intermediate samples were quickly iced and then stored at 2°C awaiting chemical analysis.

4.2.1 Reactions at 40°C

Tests performed at 40°C resulted in an absence of any significant reaction between reactants over the duration of the tests up to 137 h in some cases. Only upon using an Al:Si molar ratio of 1:1 (0.1 M Al and 0.1 M Si) did a very small amount of solids form, and analytical results of solution reactant concentrations produced nearly straight lines. Upon using a ratio of 2:1 (0.1 M Al and 0.05 M Si) at this temperature, again just nonquantifiable traces of solids were observed. At a molar ratio of 20:1 (0.1 M Al and 0.005 M Si), no solids were observed anywhere for up to 120 h. Any change in solution reactant concentrations of aluminum or silicon was within the expected analytical sensitivity. Had these tests run longer, they may have resulted in a more complete reaction. For the few tests performed at higher Al:Si ratios at this temperature, that is, Al:Si of 0.5 (0.05 M Al and 0.1 M Si) and 0.05 (0.005 M Al and 0.1 M Si), only a very small amount of solids formed on the vessel bottom at a ratio of 0.5 after 120 h. After 95 h at a ratio of 0.05, no solids were observed suspended in solution or on vessel surfaces. Generally tests performed at the lower temperature of 40°C and especially at higher Al:Si molar ratios resulted in erratic aluminum and silicon analyses for reasons not understood.

4.2.2 Reactions at 60°C

Reactions performed at 60°C produced the maximum amount of solids on both the walls and bottom of the reaction vessel at an Al:Si molar ratio of 1:1 (0.1 M Al and 0.1 M Si) after 30 h, as shown in Fig. 2. Increasing this ratio to 2:1 (0.1 M Al and 0.05 M Si) produced solids on the bottom as hard spirals only and the kinetics was diminished compared with that of the 1:1 ratio. In addition, operating at a ratio of 20:1 (0.1 M Al and 0.005 M Si) resulted in the production of a small amount of suspended solids after 47 h and no solids on vessel surfaces; desilication kinetics was also substantially slowed as expected.

At this temperature, two reactions were also performed with silicon concentrations higher than that of aluminum. Ratios of 0.5 (0.05 M Al and 0.1 M Si) and 0.05 (0.005 M Al and 0.1 M Si) were investigated. At the ratio of 0.5, solids formed on the bottom as well as on the walls, with shark-teeth-like growths after 30 h. In contrast, at a ratio of 0.05, solids formed only on the bottom after 46 h and did not adhere well. The analytical results from these tests were erratic, but it appears that at 40 and 60°C, solid deposition mirrored reactions performed at similar ratios but with aluminum in excess.

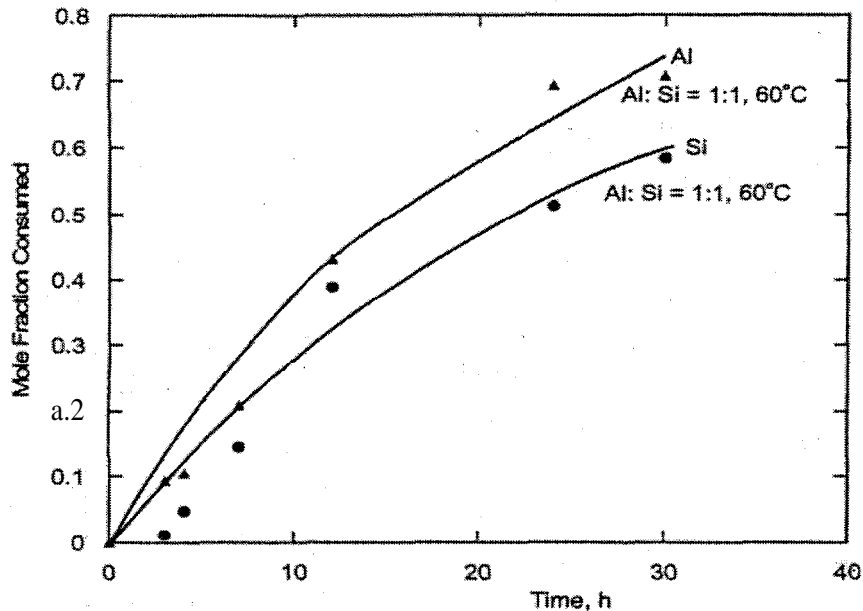


Fig. 2. Mole fraction consumption of reactants at Al:Si = 1 and 60°C.

4.2.3 Reactions at 80°C

Reactions performed at 80°C as shown in Fig. 3 demonstrate the influence of first-order dependency of the reaction kinetics on each of the reactants individually, as is often the case in overall second-order reactions. As expected, the reaction with an Al:Si ratio of 1:1 produced the highest reaction rate and largest amounts of hard solids on vessel surfaces. In the reaction with the Al:Si molar ratio of 2:1 (0.1 M Al and 0.05 M Si), the limiting reactant (Si) has been reduced by half and the results on the observed kinetics are apparent. When using an Al:Si molar ratio of 20:1 (0.1 M Al and 0.005 M Si) at this temperature, only a small amount of suspended solids was observed in solution, none on vessel surfaces, and kinetics was linear up to 30 h.

A few tests were performed at this temperature in which molar quantities of silicon were higher than those of aluminum at ratios of 0.5 (0.05 M Al and 0.1 M Si) and 0.05 (0.005 M Al and 0.1 M Si). At a ratio of 0.5, hard solids formed on the bottom and in the bulk of the solution and shark-teeth-like growths formed on the walls after 29 h. Performing the reaction at a 0.05 ratio resulted in the formation of solids only in the bulk of the solution and none on the vessel surfaces after 29 h. This reaction, based upon aluminum consumption, was 56% complete. In these reactions in which silicon concentrations exceeded aluminum concentrations, analytical results were erratic.

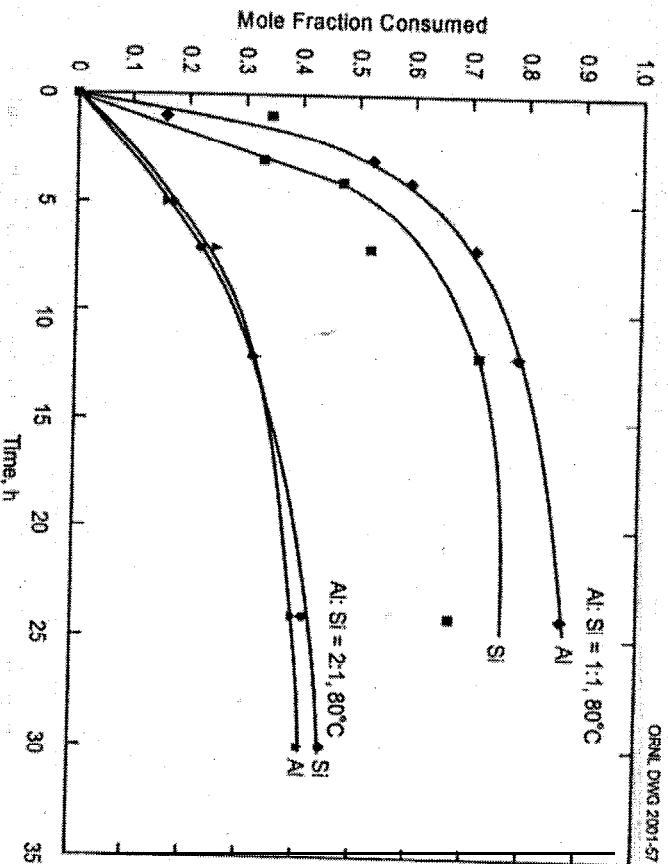


Fig. 3. Mole fraction consumption of reactants at different Al:Si ratios at 80 °C.

4.2.4 Reaction at 100 °C

The combination of a higher temperature, coupled with an Al:Si molar ratio of 1:1 (0.1 M Al and 0.1 M Si), a ratio at which desilication kinetics and solid deposition are usually at a maximum at nearly all temperatures, is provided in Fig. 4. The reaction, based upon aluminum, is approximately 90% complete after only 4 h, with the last 3 h of the reaction appearing to be at or near an equilibrium condition. Since in a pure sodalite mineral the molar ratio of Al:Si is 1, intuitively one might expect that these two curves might be closer together. Although it is possible that a solid other than sodalite may be forming to account for the separation, aluminate sorption onto silicate gel may take place at an Al:Si molar ratio greater than a 1:1.^{17,18} However, if the concentrations of both reactants during the last 3 h are used to calculate a solubility product for nitrate-based sodalite, it is very close to the literature value in this case. As shown in Figs. 2 and 3, the curves are relatively close together.

Most curves presented in this report indicate that aluminum is always consumed at a slightly greater rate than that of silicon. This is believed to occur because aluminate is adsorbing on silicate surfaces in molar ratios higher than 1:1.

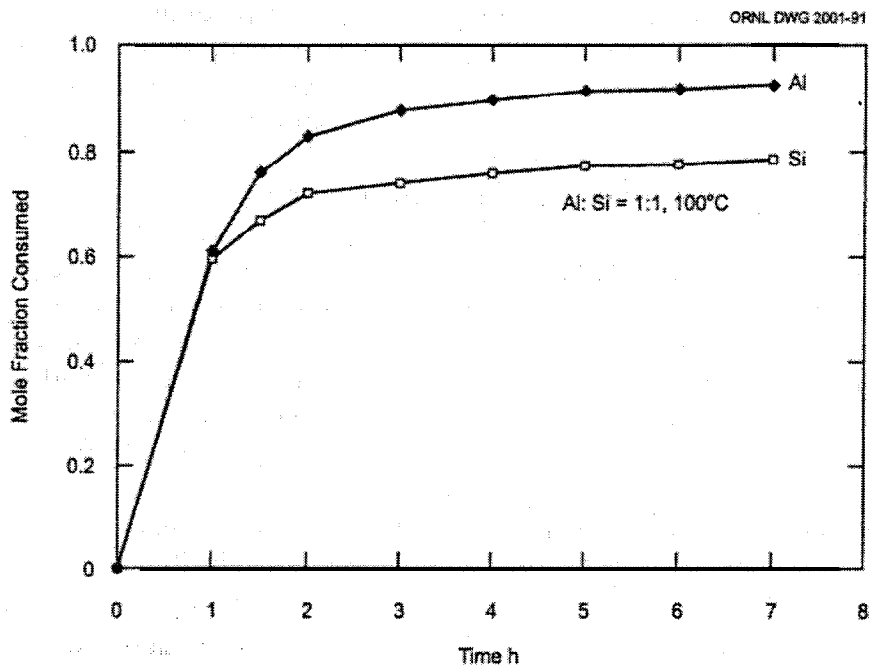


Fig. 4. Mole fraction consumption of reactants at 0.1M Al and 0.1M Si at 100°C.

4.3 TEST FOR SECOND ORDER REACTION KINETICS

Fitting experimental kinetic data to a standard integrated form for a second-order reaction in which the starting reactants are both equal can be accomplished by using the integrated form for a type II [A + B = Product] second-order reaction, as is frequently done in the literature on kinetics. If the concentrations of A and B are equal, we need not consider two terms, such as (A - X) and (B - X), but only one, (A - X)². In such situations, the rate may be expressed as

$$\frac{dx}{dt} = k(a - x)^2, \quad (2)$$

where x (mol liter⁻¹) is the amount of A that has reacted in a unit volume at time t (s), and a is the initial amount. Separation of variables and integration leads to Eq. (3).

$$\frac{x}{a(a - x)} = kt \quad (3)$$

Therefore when the term $x/a(a - x)$ (L mol⁻¹) is plotted on the ordinate and time t (s) on the abscissa, a straight line passing through zero and having a slope equal to the second-order

rate constant (k) with units of $L \text{ mol}^{-1} \text{ s}^{-1}$ will result. The half-life ($t_{1/2}$) of the reaction would be $1/k a_0$, where a_0 is the initial starting concentration. Although this integrated form of the rate equation for a type II reaction is useful when the reactant concentrations are the same, most of the SRS waste feeds have substantially higher aluminate concentrations compared with silicate; hence, kinetic data may be handled in other ways.

Although the desilication reaction is overall second order, as shown in Fig. 5, when the concentration ratios of aluminate to silicate vary by a minimum of 10 or more, handling the kinetic data as a pseudo first-order reaction can prove useful, as shown by the work of Wilmarth.¹³ In this case, the logarithm of concentration versus time may simply yield a straight line. Since the concentration of aluminum in SRS waste is approximately 50 times greater than that of silicon, the aluminum concentration will remain constant by comparison with silicon with time when forming sodalite. Hence, the kinetics could also be represented just as well as a pseudo-first order reaction. The rate constant (k) in this case would have units of reciprocal time, and $t_{1/2}$ would be equal to $0.693/k$. The values of the corresponding rate constants determined by a second-order or pseudo first-order method would therefore have different units and be different numerically; however, both would have the same limiting reactant half-life.

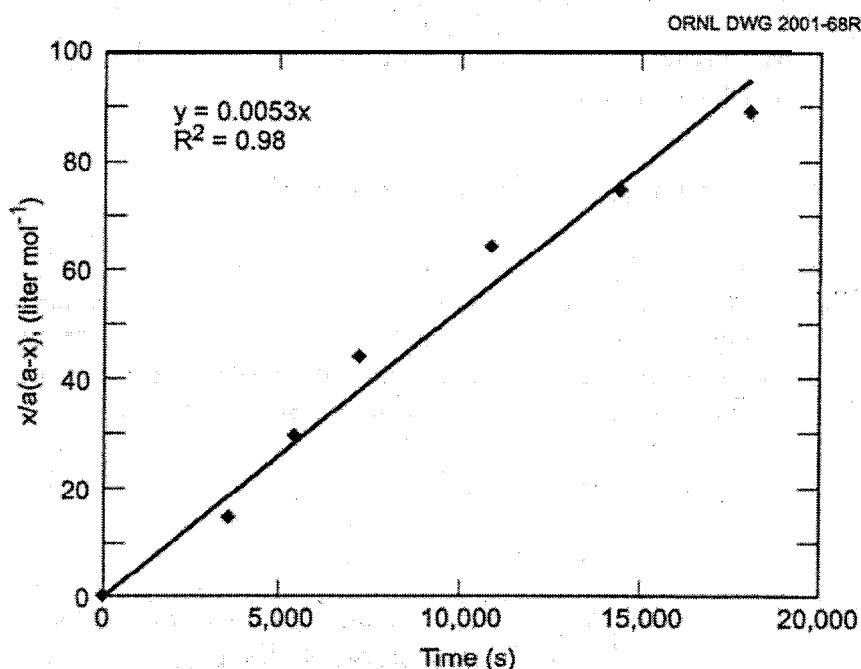


Fig. 5. Second-order reaction test plot for aluminosilicate formation at 100°C and an Al:Si molar ratio of 1:1 (0.1 M Al:0.1 M Si).

Since data presented in the Fig. 5 test plot fits the form for a second-order reaction at equal starting concentrations of reactants (0.1 M Al and 0.1 M Si), we may conclude that the

desilication reaction is overall second order. From the slope of the second-order test plot in Fig. 5, the second-order rate constant is $0.0053 \text{ L mol}^{-1} \text{ s}^{-1}$, and for a second-order reaction of this type, the half-life $t_{1/2} = 1/kA_0$, where A_0 is the initial reactant concentration. This is the amount of time that would be expected for half of this reactant concentration to decrease by 50%. It should be noted that the time for all the reactant to be completely consumed is meaningless since theoretically the time is infinite. Therefore, the half-life of the reactant is expected to be 1887 s or 0.5 h under these conditions at 100°C . This half-life is in the range of that calculated by Fondeur, Wilmarth, and Fink in the same temperature range.¹⁴ One may calculate a new specific reaction-rate constant at higher temperatures as is encountered in the 2H evaporator ($\sim 130^\circ\text{C}$), and a new associated reactant half-life as well using the modified Arrhenius equation as described below in Eq. (4).

4.4 ACTIVATION ENERGY FOR ALUMINOSILICATE CRYSTALLIZATION

From three specific reaction rate constants at three different temperatures we are able to apply the Arrhenius activation energy relationship, which relates these parameters specifically to the desilication reaction. Reactions at 60, 80, and 100°C yielded specific second-order reaction rate constants of 0.0014, 0.0022, and $0.0053 \text{ L mol}^{-1} \text{ s}^{-1}$ (see Fig. 5), respectively, which when plotted against the reciprocal of the absolute temperature yields a straight line, as shown in Fig. 6, indicating conformance to the Arrhenius relationship. The slope of the curve is -1816 K ,

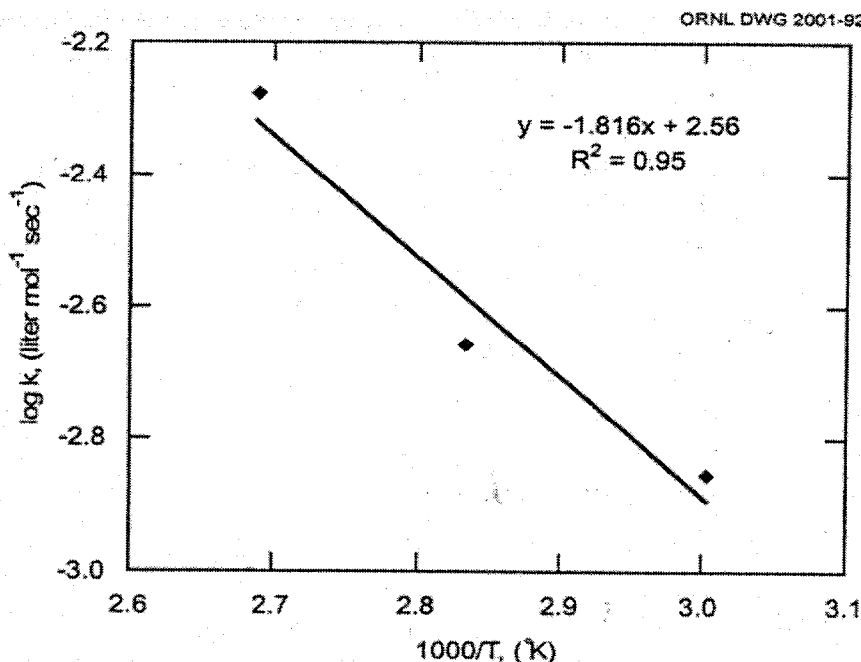


Fig. 6. Arrhenius activation energy determination for unseeded desilication reactions.

which equates to 8.31 kcal mol⁻¹ or 34.8 kJ mol⁻¹. This apparent activation energy may now be used to extrapolate specific reaction-rate constants to other temperatures provided there is no change in the reaction mechanism over the temperature range considered.

This relatively low activation energy (35 kJ mol⁻¹) means that the reaction rate will change only moderately with temperature. Those reactions that have a large activation energy will be more sensitive to a temperature change than those with a low activation energy. For example, a reaction with an activation energy of 378 kJ mol⁻¹ may increase its rate 6-fold for every 10°C near ambient temperature, while at 76 kJ mol⁻¹, the rate doubles.

It is also important to note that the solubility of the sodalite formed in these reactions is also affected by temperature and decreases modestly over the temperature range of interest in this work. For this reason, deposition on evaporator heat transfer surfaces is problematic.¹⁹

4.5 RATE CONSTANTS AT HIGHER EVAPORATOR OPERATING TEMPERATURES

It is of interest to know what the specific reaction-rate constant is at the evaporator operating temperature (~130°C) even though this work is limited by the boiling point of the 2H simulant at atmospheric pressure (~109°C). An autoclave is required to exceed the boiling point. This rate constant can be calculated using Eq. (4), where E_a is the activation energy as measured in cal mol⁻¹, R is 1.987 (cal mol⁻¹ K⁻¹), and temperature is absolute (K). Using k_2 as the second-order rate constant at 100°C or 0.0053 L mol⁻¹ s⁻¹, one may then calculate k_1 at the new temperature.

$$\log \frac{k_1}{k_2} = \frac{(T_1 - T_2)E_a}{(T_1 T_2)R} \quad 2.3 \quad (4)$$

Upon substitution in Eq. (4), the specific reaction rate constant at an evaporator operating temperature of 130°C would be 0.012 L mol⁻¹ s⁻¹. Over the temperature range of 100 to 130°C, the reaction rate would have increased by a factor of 1.25 for every 10°C rise in temperature. At a feed reactant concentration in the 2H evaporator of 0.1M, for example, a reactant half-life of 13.9 min would be expected at the specific reaction rate constant at 130°C. This is approximately half the time calculated at 100°C.

The pre-exponential factor may also be calculated from a selected temperature and its corresponding rate constant k . This pre-exponential factor (A), has been calculated to be 398 L mol⁻¹ s⁻¹. One may also calculate directly the desilication reaction rate constant at another temperature, as can also be done with Eq. (4), using the pre-exponential factor A . This factor relates the rate constant with the absolute temperature using Eq. (5),

$$k = A e^{-E_a/RT}, \quad (5)$$

where $R = 8.314 \text{ J K}^{-1} \text{ mol}^{-1}$, T is the absolute temperature of interest, and E_a is measured in J mol⁻¹. Upon substituting the value for the pre-exponential factor, one may calculate new rate

constants at other temperatures. Just as when using Eq. (4) for the same purpose, the activation energy must remain unchanged over the temperature range of interest.

4.6 REACTION INDUCTION PERIODS

In alkaline solutions containing negatively charged aluminate and silicate reactants, especially in association with water and hydroxide, initially an association between repelling anions exists that is eventually overcome by attractive induced positive charge centers formed by oxygen polarization. The partially positive aluminum and silicon centers allow electron-rich oxygen to covalently bond, eventually forming aluminosilicates. As oxygen approaches a charged center, it is slowed by steric interference, which eventually forces water out of the association. Condensation takes place as more room is made available for further interactions. The presence of other electrolytes, both positive and negative, slow this process down during the induction period by impeding diffusion of aluminate and silicate anions, which themselves tend to repel each other due to having the same charge. Heat substantially shortens the induction period by allowing water to be ejected more rapidly from a growing association or amorphous gel phase, as it is referred to. Energy imparted by heating the solution increases the Brownian motion of hydrated ions and speeds the loss of water from the gel phase, thereby increasing the rate that covalent bonds can form during condensation and nucleation.⁷

Changing the amount of aluminate present, such as when the Al:Si molar ratio is increased from 1 to 2, shows that the increase in the concentration of the similarly sized aluminate anions increases the length of the induction period at the same temperature. During this time, gel phases are losing associated water and rearranging prior to reaction. This effect on the induction period is evident from the data provided in Table 4. Reactions were also run at molar ratios of 20:1, but even after 5 days at 40 to 80°C, the reactant concentrations remained substantially unchanged. Induction periods were determined from the analytical-concentration-versus-time curves for each test.

Table 4. Desilication reaction induction periods

Al:Si ratio	Temperature (°C)	Induction period (h)
1:1	100	0
1:1	80	1
1:1	60	3-4
1:1	40	120 ^a
2:1	80	5
2:1	60	6-8
2:1	40	24-48 ^a

^a These data do not follow the trend.

The induction period ends when crystallization of a **solid** phase, such as Zeolite A or sodalite forms, thus providing a surface for continued growth at a lower energy of nucleation due to the presence of the newly generated seed. Following the appearance of a **sufficiently** seeded solution, the reaction rate increases. This delay is also partly due to the fact that the free energy associated with the formation of the mineral phase is counteracted by the high surface energy of the smallest aluminosilicate unit cell. At such a small size, the solubility of the first crystals formed can be expected to be many times more soluble than the reported mineral solubility; hence, this enhanced solubility tends to counteract the forward reaction of solids formation during this period.

4. REACTOR SCALING AND DEPOSITION OBSERVATIONS

Observations pertaining to scaling and deposition have been an extremely important aspect of this kinetic study since this is the primary condition we are trying to avoid in the 2H evaporator. Establishing the kinetics of the reactions was of secondary importance but has led to valuable observations being made during sample retrieval and at the end of each test. Generally it can be said that upon using X-ray analysis on the numerous solids formed, either filtered from the bulk of the stirred solution or 'scraped from vessel surfaces, that the nitrate-nitrite-based sodalite ultimately formed in every case. With the exception of a precursor zeolite phase which was observed and is discussed in the next section, the sodalite phase appeared to form on select surfaces, controlled to some limited degree by solution movement within the reaction vessel.

The reaction vessel (304 SS) was made from nearly the same steel as in the 2H evaporator, except for a lower carbon content in the evaporator. Additionally, the laboratory vessels used had a scoured surface with surface roughness that was probably not present in the evaporator, a condition which could have aided in the attachment of solid particles. Unlike the evaporator, the solution in the reaction vessel was constantly stirred at 250 rpm; however, as reported in the literature, mixing is said to have no effect upon the desilication reaction rate and subsequent scale deposition on steel surfaces.²⁰ However, this work has shown that mixing appears to control at least the areas where there is an apparent absence of growth, with hydrodynamics playing some role in determining where scaling will consistently be absent.

Based upon visual inspection, coupled with using a spatula on the surface to feel for a smooth or rough surface, which is quite apparent when only a small amount of scaling is present, an assessment was made. The mixer propeller pushed the solution downward, causing a spiraling pattern to form on the vessel's bottom near the outer edges of the propeller tips, with a scale-free area always immediately below the propeller. The spirals formed a type of convolute surface which rose in curved; vertical strips with a scale-free area in between and parallel, always pointing in the direction of the solution movement. Side walls in the same plane as the propeller and just above it also remained scale free, with strange growths which looked likeshark's teeth scattered randomly and sometimes extending upward to just below the solution level at times.

These strange growths were never very numerous and were found to be exclusively **sodalite**. The growths had sharp points, which pointed oddly in the direction of the on-coming solution. Such an observation might not at first seem to be very significant; however, it may provide some insight into the mechanism of growth in that fine particles impacting a growing

surface are controlled by solution movement. Direct impacts to the tip of the growing point result in the maximum transfer of kinetic energy in the moving particle, maximizing chances for attachment there, while on the slopes of this surface, the particles do not attach as well due to the glancing angle at which the particles hit. All observations made during these kinetic tests seem to support this somewhat profound observation that particles (single crystals or their agglomerations) tend to best form a scale or deposition on vessel surfaces when there is a steep angle between the surface and particle trajectory. Also particles impacting other particles, stationary or moving, tend to agglomerate or attach to each other very well. Therefore, solution hydrodynamics appears to play an important role in the location and amount of solids deposited on reaction vessel surfaces.

Of the three different Al:Si ratios and four different temperatures investigated, the maximum amount of solids formed on vessel surfaces per unit of time occurred at a molar ratio of Al:Si =1 (0.1 M Al and 0.1 M Si) at all temperatures investigated. From visual inspection, the amount deposited per unit time at this ratio appears to be at a maximum at the highest temperatures (80 and 100°C) and apparent but slower at 40°C. Since the mineral sodalite contains this molar ratio in its lattice, one can see why this might be a worst case.

4.7.1 Using Aluminum Concentrations in Excess of Silicon

The analytical concentration of aluminum and silicon in tank 43H at different levels indicates that the molar ratios of Al:Si are amazingly constant at a ratio of 50: 1.¹⁵ In this study, we have usually maintained an excess of aluminum with a maximum Al:Si molar ratio of 29: 1.

As previously stated, the maximum rate of solids deposition on vessel surfaces occurred at an Al:Si molar ratio of 1 with the deposition rate, based upon visual inspection, highest at 80°C and 100°C and lowest at 40°C. At a molar ratio of 2:1 (0.1 M Al and 0.05 M Si), the bulk of the solids favored deposition on the bottom of the vessel at the higher temperatures (60 and 80°C), while at 40°C, deposition was more pronounced on the wall than the bottom; the reason for this is unclear. In addition, for tests performed at ratios of 20: 1, no scale formation was observed at all at any temperature over 2 to 5 days of testing. As discussed previously, the reason for this is believed to be due in part to the concentrations at this molar ratio (0.1 M Al and 0.005 M Si) (neglecting activity coefficients) being close to the solubility product for the sodalite, depending upon the literature value chosen; therefore, the mass action driving force is low.

4.7.2 Using Silicon Concentrations in Excess of Aluminum

Six tests were performed in which the amount of silicon exceeded that of aluminum. These few tests yielded some analytical results for silicon that were especially poor, and results did not lend themselves well to kinetic interpretation. Results did, however, show that at an Al:Si molar ratio of 0.05 (0.005 M Al and 0.1 M Si), no measurable reaction between aluminate and silicate occurred over 4 days at 40°C. Using the same ratio at 60°C resulted in some solids forming only on the bottom of the vessel; these solids did not adhere well to the vessel after 4 days. Upon repeating this test with a molar ratio of 0.05 and again at 80°C, solids only formed

in the bulk of the solution and not on vessel surfaces at all after 29 h. Analytical results for silicon were erratic, but aluminum results were good and indicated that approximately 56% of the aluminum had been removed from the solution.

Tests performed at Al:Si ratios of 0.5 (0.05 M Al and 0.1 A4 Si) at 40°C yielded solids which only formed on the bottom of the vessel after 5 days and were very firmly attached. Duplicating this test at 60°C again showed the formation of solid on the bottom and numerous shark's teeth on the walls after 30 h. Again duplicating this test at 80°C and at the same molar ratio, it was found, based on the aluminum analytical results, that 98.6% of the aluminum had been removed from the solution. In this case the bulk of the solution contained solids, but most solids formed a hard, well-adhering scale with a soft, nonsticking layer above on the bottom of the vessel.

4.8 ZEOLITE A PRECURSOR PHASE

There has been speculation regarding which mineral phase may form as a precursor to the formation of sodalite both in the bulk solution as well as on vessel walls.¹² Knowing the identity of the precursor phase could theoretically allow for some control over the conditions which favor or impede the formation of the precursor phase and thereby aid in controlling sodalite formation.²¹ Throughout this work, nearly all solids formed, whether in the bulk of the solution or attached to vessel surfaces, have been shown to be the nitrate-nitrite-based sodalite [46-0730]. The intercalation of both nitrate and nitrite has been reported by Buhl.²²

Only on two occasions was the presence of Zeolite A indicated. The XRD spectra in Fig. 7 shows that the solids filtered from the bulk of the solution in a test at 80 °C and Al:Si = 1 were initially Zeolite A during the first 2 h and then were converted to the nitrate-nitrite-based sodalite starting at 3 h. According to Breuer, this conversion is expected to occur at 70°C and above, and is enhanced by high alkalinity.²³ Additionally, Zheng et al., also reports, based upon sodalite formation results obtained at temperatures between 70 to 100°C, that initially crystallized zeolite transforms to sodalite.²⁴

In a test at 40°C and at the same Al:Si molar ratio, Zeolite A was also found in solid scraped from reactor vessel walls. It is possible that the conversion from Zeolite A to the sodalite extends to the lower temperature where it is much slower. Because the conversion rate may have been so much slower at 40°C, we were unable to see it using XRD.

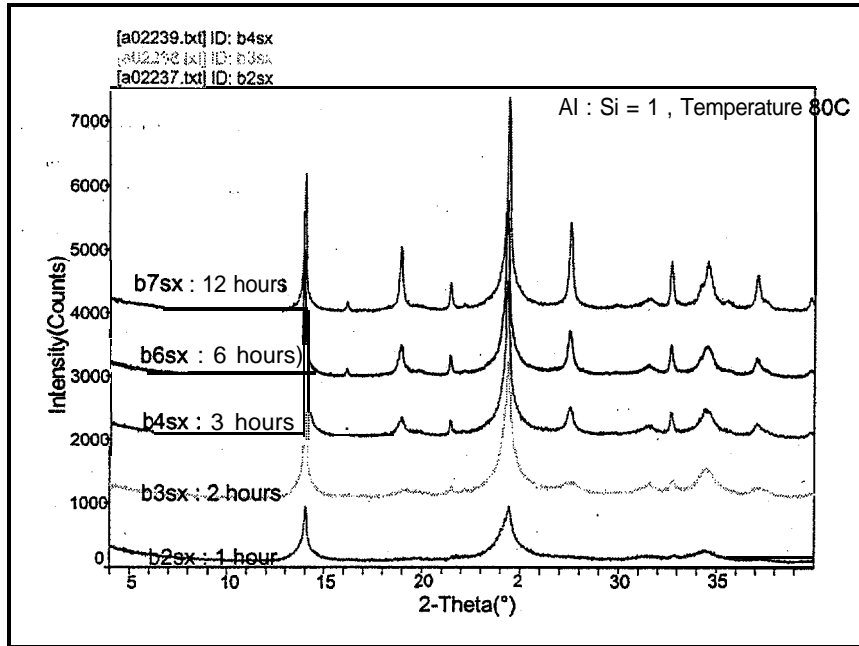


Fig. 7. XRD spectra showing the conversion of Zeolite A into nitrate-based sodalite.

4.9 USING CARBON BLACK AS A SEED

During this phase of the investigation, an effort was made to take advantage of the well-known ability of seed material to lower the free energy associated with heterogeneous nucleation and therefore speed the rate of formation of the sodalite in the bulk solution. In the case of heterogeneous nucleation, the presence of a foreign surface can lower the overall free energy change associated with the formation of a critical nucleus; that is,

$$\Delta G_{crit,het} = \Phi \Delta G_{crit,hom} \quad (6)$$

The quantity Φ is less than 1, and it takes into account the reduction in ΔG due to participation of foreign surfaces in the nucleation process, where

$$\Phi = [(2 + \cos\alpha)(1 - \cos\alpha)^2] / 4 \quad (7)$$

and α , the contact angle between the deposit and the foreign solid surface, becomes a measure of the affinity between the nuclei and the foreign solid surface.²⁵ Normally one would expect to

choose a solid surface which is not only crystalline but perhaps composed of the expected mineral phase formed during desilication—in this case sodalite or a similar homolog. The enhancement in reaction rate in bulk solution due to the use of seed material has already been investigated and proven throughout the literature.^{20, 26-30} According to Barnes et al., “the desilication rate was observed to increase dramatically due to seed crystal growth with the suppression of scale formation.”²⁰ This approach to scale control based upon seeding is used effectively in both the United States and in Russia. According to the Kirk-Othmer encyclopedia, “the second approach, the so-called seeding technique, provides preferential sites for the nucleation of scale which permits the heat-transfer surfaces to remain clean of scale.” Field use in Russia was reported in the mid-1960s and by all of the Resources Conservation Company’s (Bellevue, Washington) vapor-compression units in the United States.^{9, 31}

Carbon black, sometimes called lamp black or Paris black, is a major component of tires and also newspaper printing ink and has a surface area of up to as much as 1100 m²/g. It is not a crystalline material, but it is sometimes called polycrystalline (nongraphitic) due to hexagonal-shaped pairing of particles in random directions and with nonuniform lattice spacing in small crystallites in an amorphous carbon bulk. However, its potential to be oxidized to CO₂ in the cold cap of the glass melter made it an attractive material to try as a seed. In a single test at 80°C and Al:Si = 1, the carbon was used at 2.4 kg/1000 L of simulant feed. This was very likely much more carbon than was needed as a suitable seed. The carbon was used without adding any wetting agents to it, and after 5 min the floating carbon was wetted by the hot solution and remained dispersed.

After 6 h, the test was ended and it was found that most of the low-density carbon collected at the bottom of the vessel when mixing was halted. Although pure carbon has a density of 2.26 gm/cc, carbon black has 40% void space which lowers its density to about 1.3 gm/cc, which is close to that of the simulant.³² The walls of the vessel at this temperature and Al:Si ratio normally appear to be coated with the maximum amount of solid, especially on the bottom of the vessel and cannot be scraped off. Following the use of carbon black, the walls as well as the bottom of the vessel were clean to the naked eye.

The scanning electron micrographs (SEMs) of the solids that form at the bottom are shown in Figs. 8 and 9. Carbon taken from the bottom of the reaction vessel shows the characteristic yarn-like balls of sodalite attached to the shapeless surfaces of the carbon, which have more rounded edges (Fig. 8). For comparative purposes, Fig. 9 shows the rather shapeless carbon black not used in the reaction.

Because of experimental conservatism, this first test of using carbon black as a crystallization seed employed far more carbon black than was probably needed. For this reason, the photomicrograph in Fig. 9 is overwhelmed by much of the shapeless carbon mass at this magnification. The solids shown in the figure were washed with very large volumes of water and were combined with soaking overnight to ensure that simulant salt crystals would not be present.

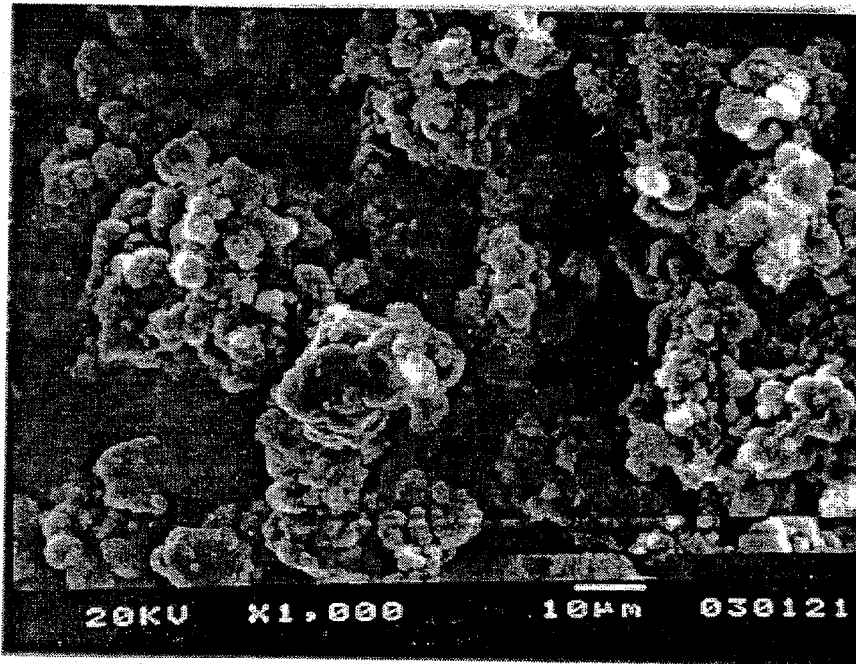


Fig. 8. SEM photomicrograph showing sodalite growth on carbon black surfaces.

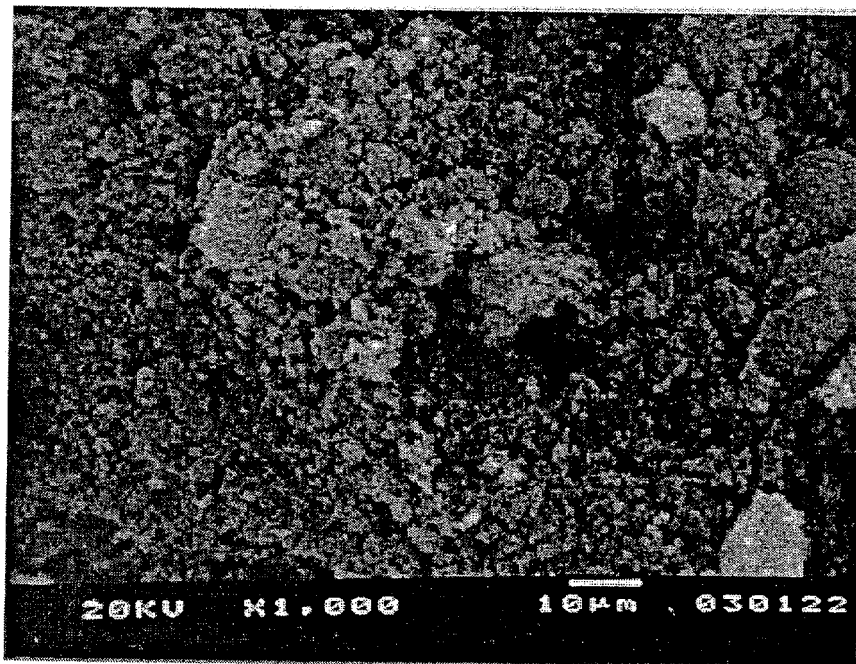


Fig. 9. SEM photomicrograph of unused carbon black.

4.10 A KINETIC TEST AT 100°C

Although this phase of the work focused on the temperature range of 40 to 80°C, a single test was performed at 100°C and at an Al:Si ratio of 1; that is, both aluminum and silicon were initially at 0.1 M. For this test, the water in the bath was replaced with silicon oil, which allows work closer to the boiling point of this simulant (~109°C) at atmospheric pressure to be performed. In addition, the 20-mL sample bottles receiving the intermediate samples were placed in an ice bath. These samples were stored in ice until the end of the 7-h test, at that time they were moved to a refrigerator until being analyzed by ICP. This was done to ensure that the samples removed would be less likely to continue to react while awaiting chemical analysis.

As one might predict, the kinetics of desilication was much faster at this higher temperature, and unlike other tests, no induction period was present during the early stage of the reaction. The curves of concentration versus time are shown in Fig. 10, with an apparent approach to equilibrium revealed between the solid phase and the solution aluminate and silicate concentration during the last 3 h. At this temperature and under these conditions the reaction appears to have been completed in 4 h.

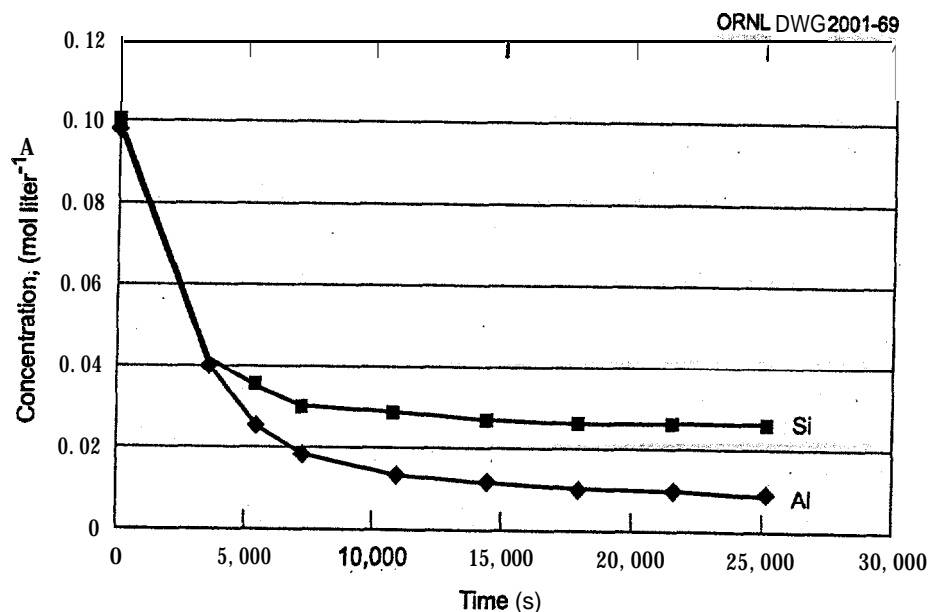


Fig. 10. Concentration versus time for a reaction at 100°C (Al:Si=1) showing an approach to equilibrium after 4 h.

If we assume that an equilibrium is achieved during the last 3 h of the 100°C reaction, then from the analytical concentrations of aluminate and silicate we can calculate a solubility product at this temperature and ionic strength. From the solution concentrations during the last 3 h, neglecting activity coefficients, we calculate a solubility product (k_{sp}) of $2.6 \pm 0.1 \times 10^{-4} M^2/L^2$ for the nitrate-nitrite-sodalite, which appears to be within the acceptable range of published values at this temperature.^{33, 34}

5. CONCLUSIONS

Desilication kinetics of the Savannah River 2H evaporator simulant exhibited second-order kinetics with a maximum rate of nitrate-nitrite-based sodalite formation at the highest temperatures and at Al:Si molar ratios of 1: 1 (0.1 M Al and 0.1 M Si), corresponding to the same molar ratio present in the sodalite mineral. A second-order reaction rate constant was extrapolated to the 2H evaporator operating temperature (-130°C) and was found to be $0.012 L mol^{-1} s^{-1}$, which would correspond to a reactant half-life in the evaporator of 13.9 min, assuming a 0.1 M feed. The apparent Arrhenius activation energy for the formation of the crystalline sodalite was found to be 35 kJ/mol.

Desilication reactions performed at Al:Si molar ratios as high as 20: 1, regardless of the temperature, were slow by comparison with other conditions investigated. Even after 130 h, no change in reactant concentrations could be observed within the inherent analytical sensitivity. This may have been due in part to the fact that we chose to operate close to the solubility limit for the sodalite mineral, depending upon the literature value considered. From a single test conducted at 100°C and an Al:Si molar ratio of 1:1, a solubility product for the nitrate-nitrite-based sodalite formed was found to be $2.6 \pm 0.1 \times 10^{-4} M^2/L^2$ at this temperature and ionic strength.

Tests were also performed in which the concentration of silicon was higher than that of aluminum at Al:Si ratios of 0.5 and 0.05 and at temperatures of 40, 60, and 80°C. It was found that under most of these conditions, solids formed on vessel surfaces except at the maximum temperature and when silicate concentrations were highest compared with aluminate. In one test at an Al:Si molar ratio of 0.05 (0.005 M Al and 0.1 M Si), or equivalent to a Si:Al ratio of 20: 1, at 80°C produced solids only in the bulk of the solution and no visual trace of solid formation on vessel surfaces. This reaction consumed 56% of the available aluminum over 29 h. Although only a single test produced these results, high Al:Si ratios at high temperatures will be considered during the next phase of testing.

Throughout this work, the predominant aluminosilicate solid identified by XRD, either in the bulk solution or adhering to reaction vessel surfaces, was a nitrate-nitrite-based sodalite. Once formed, this solid adhered to the polished steel surfaces of the 304-L SS reaction vessels such that removal was always very difficult, requiring the use of sulfuric acid to remove it. In all tests, based upon visual inspection and the use of a scraper to check for solids, the wall surface in the same plane as the propeller and just above it always remained free of scale or deposition. In addition, the area directly below the propeller, which always operated at 250 rpm, also remained

free of any scale or deposition. The reason for this is likely related to solution hydrodynamics and therefore particle movement profiles within the stirred reaction vessel.

Observations made during the course of this work have consistently shown that in areas where particles impact the metal surface more directly (at a steeper angle) and with presumably higher kinetic energy imparted by the mixer blade and solution, adherence to the surface becomes more pronounced. In addition, surface-adhering particles appear to grow laterally across the surface, forming a thin sheet of solid which can then build new layers. It also appears that particles (crystals) that impact each other agglomerate and form a sheet which may stand vertically on the surface in parallel layers with space in between. The vertical layers follow the direction of the expected solution movement, forming uniform spirals, especially on the vessels bottom, at the outside edge of the mixer propeller. This observation can lead one to speculate that a sodalite crystal, once formed, may be coated by a **diffuse** gel-like layer that feeds crystal growth but also acts like a **"glue"** to facilitate agglomeration upon particle-particle impact and with similarly coated vessel surfaces.

Although most XRD analyses of the aluminosilicates that formed proved to be the **nitrate-nitrite-based** sodalite, a search for an expected precursor solid such as gibbsite or a zeolite during two different tests revealed that Linde Zeolite A formed first and was then converted to the sodalite. Although this conversion is known to occur at temperatures of 70°C and above from the literature, some Zeolite A was found on reactor vessel walls at 40°C with an Al:Si ratio of 1:1. In addition, samples of solids formed in solution over the first 3 h of a test at 80°C, and at the same Al:Si ratio, revealed that Zeolite A was forming initially in solution and then converting to the sodalite mineral after 3 h, as proven by XRD analyses. If this is the only solid precursor to the formation of problematic sodalite, and if the reaction pathway must include its metastable formation, then perhaps efforts directed at destabilizing its formation might prove useful.

A single test **was** performed near the end of this phase of the experimental work using carbon **black**, a material present in tires and newsprint ink, as a seed material to promote the formation of sodalite more rapidly in the bulk of the solution rather than on vessel surfaces. This test was performed at a temperature of 80 °C and an Al:Si molar ratio of 1: 1, which are the conditions where fast kinetics and the maximum surface deposition occur. Although much more carbon was used than was likely necessary (equivalent to 2.4 kg/1 000 L of solution), no solids formed on the vessel walls and the carbon black with attached mineralization collected on the bottom of the reaction vessel. This material would likely be oxidized in the cold cap region of the glass melter to CO, and hence was of interest as one of a number of potential seed materials.

6. RECOMMENDATIONS

Keeping in mind that the results of these studies are based on only a few experiments, two possible approaches were identified that could lead to the elimination of evaporator scaling problems — the use of higher **Si:Al** ratios in the feed solution and the use of seeds to promote bulk solution precipitation, perhaps using carbon-black seeded reactions.

7. REFERENCES

1. R. D. Hunt, T. A. Dillow, J. R. Parrott, J. R., J. C. Schryver, C. F. Weber, and T. D. Welch, *Waste Preparation and Transport Chemistry: Results of the FY 2000 Studies*, ORNL/TM-2000/298, December 2000.
2. W. R. Wilmarth and S. D. Fink, *Evaporator Cleaning Studies*, Westinghouse Savannah River Company, Aiken, S.C., WSRTC-TR-98-00406, Rev. 0, Nov. 16, 1998.
3. W. R. Wilmarth, *Comparison of Nitric Acid and Sulfuric Acid Dissolution of Samples from the 242-1 6H Evaporator Pot*, Westinghouse Savannah River Company, Aiken, S.C., WSRC-TR-2000-00209, July 10, 2000.
4. W. R. Wilmarth, C. J. Coleman, J. C. Hart, and W. T. Boyce, *Characterization of Samples from the 242-1 6H Evaporator Wall*, Westinghouse Savannah River Company, Aiken, S.C., WSRC-TR-2000-00089, Mar. 20, 2000.
5. C. S. Boley, M. C. Thompson, and W. R. Wilmarth, *Technical Basis for the 242-16H Evaporator Cleaning Flowsheet*, Westinghouse Savannah River Company, Aiken, S.C., WSRC-TR-2000-00211, July 12, 2000.
6. R. A. Peterson and R. A. Pierce, *Sodium Diuranate and Sodium Aluminosilicate Precipitation Testing Results*, Westinghouse Savannah River Company, Aiken, S.C., WSRC-TR-2000-00156, Oct. 30, 2000.
7. S. Ostap, "Control of Silica in the Bayer Process Used in Alumina Production,," *Canadian Institute of Mining and Metallurgy* **25(2)**, 101-106 (1986).
8. K. Yamada, M. Yoshihara, and S. Tasaka, "Properties of Scale in Bayer Process," in *Light Metals 1985*, R. E. Miller, editor, The Metallurgical Society, Inc., Proceedings of the TMS Light Metal Committee at the 114th Annual Meeting, New Orleans, Louisiana, pp. 223-235, Feb. 24-28, 1985.
9. Kirk-Othmer, pp. 346-348 in *Encyclopedia of Chemical Technology*, vol. 24, 3rd edition, Wiley, N.Y., 1978.
10. G. A. Cappeline et al, *Drew Principles of Industrial Water Treatment*, LOC number 77-76610, Drew Chemical Corp., Boonton, N.J., 2nd edition, 1978.
11. Lee Dworjany, personal communication, Westinghouse Savannah River Company, Aiken, S.C., March 2001.

12. C. M. Jantzen, and J. E. Laurinat, *Thermodynamic Modeling of Deposition in Savannah River Site (SRS) Evaporators*, WSRC-TR-2000-00293; Westinghouse Savannah River Company, Aiken, S.C., Aug. 30, 2000.
13. W. R. Wilmarth, D. D. Walker, and S. D. Fink, *Sodium Aluminosilicate Formation in Tank 43H Simulants*, Westinghouse Savannah River Company, Aiken, S.C., WSRC-TR-97-00389, Nov. 15, 1997.
14. F. F. Fondeur, W. R. Wilmarth, and S. D. Fink, *Calculation of the Aluminosilicate Half-Life Formation Time in the 2H Evaporator*, Westinghouse Savannah River Company, Aiken, S.C., WSRC-TR-2000-00267, July 28, 2000.
15. W. R. Wilmarth, and R. A. Peterson, R.A., *Analyses of Surface and Variable Depth Samples from Tank 43H*, Westinghouse Savannah River Company, Aiken, S.C., WSRC-TR-2000-00208, Mar. 16, 2001.
16. F. D. Snell, and L. S. Ettre, *Encyclopedia of Industrial Chemical Analysis, Analysis of Commercial Sodium Silicate Solutions*, vol. 18, Interscience Publishers, N.Y., 1973.
17. R. D. Hond, "Alumina Yield in the Bayer Process," pp. 125-130 in *Light Metals 1986*, R.E. Miller, editor, The Metallurgical Society, Inc., Proceedings of the TMS Light Metal Committee at the 115th Annual Meeting, New Orleans, Louisiana, Mar. 2-6, 1986.
18. E. C. Beahm, C. F. Weber et al, *Sludge Treatment Studies, Oak Ridge National Laboratory, Oak Ridge, TN, ORNL/TM-13371*, June 1997.
19. H. Muller-Steinhagen, M. Jamialahmadi, and B. Robson, "Understanding and Mitigating Heat Exchanger Fouling in Bauxite Refineries," *Journal of Metals*, **46**, 36-41, Nov. 1994.
20. M. C. Barnes, J. Addai-Mensah, and A. R. Gerson, "The Kinetics of Desilication of Synthetic Spent Bayer Liquor and Sodalite Crystal Growth," *Colloids and Surfaces A: Physicochemical and Engineering Aspects* **147**, 283-295 (1999).
21. S. Bosnar, and B. Subotic, "Mechanism and Kinetics of the Growth of Zeolite Microcrystals Part 1: Influence of the Alkalinity of the System on the Growth Kinetics of Zeolite A Microcrystals," *Microporous and Mesoporous Materials* **28**, 483-493 (1999).
22. J.-C. Buhl, and J. Lons, "Synthesis and Crystal Structure of Nitrate Enclathrated Sodalite- $\text{Na}_8[\text{AlSiO}_4]_6(\text{NO}_3)_2$," *Journal of Alloys and Compounds* **235**, 41-47 (1996).
23. R. G. Breuer, L. R. Barsotti, and A. C. Kelly, "Behavior of Silica in Sodium Aluminate Solutions," pp. 133-157 in *Metallurgy of Aluminum*, vol. 1, Interscience, N.Y., 1963.

24. K. Zheng, A. R. Gerson, J. Addai-Mensah, and R. St. C. Smart, "The Influence of Sodium Carbonate on Sodium Aluminosilicate **Crystallisation** and Solubility in Sodium Aluminate Solutions," *Journal of Crystal Growth* **171**, 197-208 (1997).
25. B. Shi, and R. W. Rousseau, "Crystal Properties and Nucleation Kinetics from Aqueous Solutions of Na_2CO_3 and Na_2SO_4 ," *Ind. Eng. Chem. Res.* **40**, 1541-1547 (2001).
26. M. C. Barnes, J. Addai-Mensah, and A. R. Gerson, "The Kinetics of Desilication of Synthetic Spent Bayer Liquor Seeded with Cancrinite and Cancrinite/Sodalite **Mixed-Phase Crystals**," *Journal of Crystal Growth* **200**, 251-264 (1999).
27. A. R. Gerson, J. A. Counter, and D. J. Cookson, "Influence of Solution Constituents, Solution Conditioning and Seeding on the Crystalline Phase of Aluminum Hydroxide Using In Situ X-ray Diffraction," *Journal of Crystal Growth* **160**, 346-354 (1996).
28. K. Zheng, R. C. Smart, J. Addai-Mensah, and A. R. Gerson, "Solubility of Sodium Aluminosilicates in Synthetic Bayer Liquor," *J. Chem. Eng. Data* **43**, 312-317 (1998).
29. K. Kato, T. Yoshioka, and A. Okuwaki, "Study for Recycling of Ceria-based Glass Polishing Powder II-Recovery of Hydroxysodalite from the Alkali Waste Solution Containing SiO_2 and Al_2O_3 ," *Ind. Eng. Chem. Res.* **39**, 4148-4151 (2000).
30. M. C. Barnes, J. Addai-Mensah, and A. R. Gerson, "The Solubility of Sodalite and Cancrinite in Synthetic Spent Bayer Liquor," *Colloids and Surfaces A: Physicochemical and Engineering Aspects* **157**, 101-116 (1999).
31. V. B. Cherozubov et al., *Proceedings of the 1st International Symposium on Water Desalination*, Washington, DC., p. 139, October 1965.
32. L. C. F. Blackman, p. 35-36 in *Modern Aspects of Graphite Technology*, Academic Press, N.Y., 1970.
33. H. A. Gasteiger, W. J. Frederick, and R. C. Streisel, "Solubility of Aluminosilicates in Alkaline Solutions and a Thermodynamic Equilibrium Model," *Ind. Eng. Chem. Res.* **31**, 1183 (1992).
34. W. R. Wilmarth, and R. A. Peterson, *Analyses of Surfaces and Variable Depth Samples from Tanks 30H and 32H*, Westinghouse Savannah River Company, Aiken, S.C., WSRC-TR-2000-00112, Mar. 16, 2000.

INTERNAL DISTRIBUTION

- | | |
|---------------------|-------------------------------------|
| 1. V. F. de Almeida | 22. S. M. Robinson |
| 2-6. D. A. Bostick | 23. C. Tsouris |
| 7-11. D. W. DePaoli | 24. J. S. Watson |
| 12-16. M. Z. Hu | 25. C. F. W e b e r |
| 17. R. D. Hunt | 26. T. D. Welch |
| 18. R. T. Jubin | 27. Central Research Library |
| 19. A. J. Mattus | 28. ORNL Laboratory Records-RC |
| 20. C. P. McGinnis | 29-30. ORNL Laboratory Records-OSTI |
| 21. L. E. McNeese | |

EXTERNAL DISTRIBUTION

31. C. S. Boley, Westinghouse Savannah River Company, Building 703-H, Room 137, Aiken, SC 29808
32. T. E. Britt, Westinghouse Savannah River Company, Building 703-H, Room 85, Aiken, SC 29808
33. L. D. Bustard, Sandia National Laboratories, P.O. Box 5800, MS: 0728, Albuquerque, NM 87185 - 5800
34. E. J. Cruz, U.S. Department of Energy, Richland Operations Office, P.O. Box 550, MSIN H6-60, Richland, WA 99352
35. P. D. d'Entremont, Westinghouse Savannah River Company, Building 703-H, Room 97, Aiken, SC 29808
36. Kurt Gerdes, Tanks Focus Area Headquarters Program Lead, DOE Office of Science and Technology, 19901 Germantown Rd., 1154 Cloverleaf Building, Germantown, MD 20874-1290
37. P. W. Gibbons, Numatec Hanford Corporation, P.O. Box 1970, MS: H5-61, Richland, WA 99352
38. T. S. Gutmann, U.S. Department of Energy, Savannah River Operations Office, P.O. Box A, Aiken, SC 29802

39. E. W. Holtzscheiter, Westinghouse Savannah River Company, Savannah River Technology Center, Building 773-A, Room A-229, MS: 28, Aiken, SC 29802
40. J. O. Honeyman, Lockheed Martin Hanford Corporation, P.O. Box 1500, MS: G3-21, Richland, WA 99352
41. B. L. Lewis, Westinghouse Savannah River Company, Building 703-H, Room 99, Aiken, SC 29808
42. K. A. Lockie, U.S. Department of Energy, Idaho Operations Office, 750 DOE Place, MS: 1145, Idaho Falls, ID 83402
43. J. P. Morin, Westinghouse Savannah River Company, Savannah River Technology Center, Building 703-H Aiken, SC 29808
44. J. R. Noble-Dial, U.S. Department of Energy, Oak Ridge Operations Office, P.O. Box 2001, Oak Ridge, TN 37830-8620
45. J. F. Ortaldo, Westinghouse Savannah River Company, Building 704-S, Room 13, Aiken, SC 29808
46. Lynne Roeder-Smith, Tanks Focus Area Technical Team Communications, Pacific Northwest National Laboratory, P.O. Box 999, MSIN: K9-69, Richland, WA 99352
47. W. L. Tamosaitis, Savannah River Technology Center, Westinghouse Savannah River Company, Bldg. 773-A, Room A-23 1, Aiken, SC 29808
48. M. T. Terry, Los Alamos National Laboratory, P.O. Box 999, K9-69, Richland, WA 99352
49. T. R. Thomas, Lockheed Martin Idaho Technologies Company, P.O. Box 1625, MSIN: 3458, Idaho Falls, ID 83415-3423
50. J. H. Valentine, Bechtel BWXT Idaho, Inc., P.O. Box 1625, MS: 3211, Idaho Falls, ID 83415-3100
51. W. B. Van Pelt, Westinghouse Savannah River Company, Building 773-42A, Room 121, Aiken, SC 29808
52. W. R. Wilmarth, Westinghouse Savannah River Company, Building 773-42A, Room 153, Aiken, SC 29808
53. Tanks Focus Area Program Office, c/o T. Pietrok, U.S. Department of Energy, Richland Operations Office, P.O. Box 550, MS: K8-50, Richland, WA 99352

ology

54. Tanks FOCUS Area Program Office, c/o B. J. Williams, Pacific Northwest National Laboratory, P.O. Box 999, MSIN: K9-69, Richland, WA 99352

en,

inter,

ken,

D

121,

i
153,

nd

INTERNAL DISTRIBUTION

- | | |
|---------------------|-------------------------------------|
| 1. V. F. de Almeida | 22. S. M. Robinson |
| 2-6. D. A. Bostick | 23. C. Tsouris |
| 7-11. D. W. DePaoli | 24. J. S. Watson |
| 12-16. M. Z. Hu | 25. C. F. Weber |
| 17. R. D. Hunt | 26. T. D. Welch |
| 18. R. T. Jubin | 27. Central Research Library |
| 19. A. J. Mattus | 28. ORNL Laboratory Records-RC |
| 20. C. P. McGinnis | 29-30. ORNL Laboratory Records-OSTX |
| 21. L. E. McNeese | |

EXTERNAL DISTRIBUTION

31. C. S. Boley, Westinghouse Savannah River Company, Building 703-H, Room 137, Aiken, SC 29808
32. T. E. Britt, Westinghouse Savannah River Company, Building 703-H, Room 85, Aiken, SC 29808
33. L. D. Bustard, Sandia National Laboratories, P.O. Box 5800, MS: 0728, Albuquerque, NM 87185 - 5800
34. E. J. Cruz, U.S. Department of Energy, Richland Operations Office, P.O. Box 550, MSIN H6-60, Richland, WA 99352
35. P. D. d'Entremont, Westinghouse Savannah River Company, Building 703-H, Room 97, Aiken, SC 29808
36. Kurt Gerdes, Tanks Focus Area Headquarters Program Lead, DOE Office of Science and Technology, 1990 1 Germantown Rd., 1154 Cloverleaf Building, Germantown MD 20874-1290
37. P. W. Gibbons, Numatec Hanford Corporation, P.O. Box 1970, MS: H5-61, Richland, WA 99352
38. T. S. Gutmann, U.S. Department of Energy, Savannah River Operations Office, P.O. Box A, Aiken, SC 29802

39. E. W. Holtzscheiter, Westinghouse Savannah River Company, Savannah River Technology Center, Building 773-A, Room A-229, MS: 28, Aiken, SC 29802
40. J. O. Honeyman, Lockheed Martin Hanford Corporation, P.O. Box 1500, MS: G3-21, Richland, WA 99352
41. B. L. Lewis, Westinghouse Savannah River Company, Building 703-H, Room 99, Aiken, SC 29808
42. K. A. Lockie, U.S. Department of Energy, Idaho Operations Office, 750 DOE Place, MS: 1145, Idaho Falls, ID 83402
43. J. P. Morin, Westinghouse Savannah River Company, Savannah River Technology Center, Building 703-H Aiken, SC 29808
44. J. R. Noble-Dial, US. Department of Energy, Oak Ridge Operations Office, P.O. Box 2001, Oak Ridge, TN 37830-8620
45. J. F. Ortaldo, /Westinghouse Savannah River Company, Building 704-S, Room 13, Aiken, SC 29808
46. Lynne Roeder-Smith, Tanks Focus Area Technical Team Communications, Pacific Northwest National Laboratory, P.O. Box 999, MSIN: K9-69, Richland, WA 99352
- 4 7 . W. L. Tamosaitis, Savannah River Technology Center, Westinghouse Savannah River Company, Bldg.773-A, Room A-23 1, Aiken, SC 29808
48. M. T. Terry, Los Alamos National Laboratory, P.O. Box 999, K9-69, Richland, WA 99352
49. T. R. Thomas, Lockheed Martin Idaho Technologies Company, P.O. Box 1625, MSIN: 3458, Idaho Falls, ID 83415-3423
50. J. H. Valentine, Bechtel BWXT Idaho, Inc., P.O. Box 1625, MS: 3211, Idaho Falls, ID 83415-3100
51. W. B. Van Pelt, Westinghouse Savannah River Company, Building 773-42A, Room 121, Aiken, SC 29808
52. W. R. Wilmarth, Westinghouse Savannah River Company, Building 773-42A, Room 153, Aiken, SC 29808
53. Tanks Focus Area Program Office, c/o T. Pietrok, U.S. Department of Energy, Richland Operations Office, P.O. Box 550, MS: K8-50, Richland, WA 99352

54. Tanks Focus Area Program Office, c/o B. J. Williams, Pacific Northwest National Laboratory, P.O. Box 999, MSIN: K9-69, Richland, WA 99352

ology

en,

nter,

ken,

D

121,

153,

ind